Origin of the Okubo-Zweig-Iizuka rule in QCD

Nathan Isgur
Jefferson Laboratory, 12000 Jefferson Avenue, Newport News, Virginia 23606

H. B. Thacker
Department of Physics, University of Virginia, Charlottesville, Virginia 22901

(Received 12 May 2000; revised manuscript received 10 July 2001; published 9 October 2001)

The Okubo-Zweig-Iizuka (OZI) rule is prominent in hadronic phenomena only because OZI violation is typically an order of magnitude smaller than expected from large N_c arguments. With its standard $^3P_0$ pair creation operator for hadronic decays by flux tube breaking, the quark model respects the OZI rule at the tree level and exhibits the cancellations between OZI-violating meson loop diagrams required for this dramatic suppression. However, if the quark model explanation for these cancellations is correct, then OZI violation would be expected to be large in the nonet with the same quantum numbers as the pair creation operator: the 0^{++} mesons. Experiment is currently unable to identify these mesons, but we report here on a lattice QCD calculation which confirms that the OZI rule arises from QCD in the vector and axial vector mesons as observed, and finds a large violation of the rule in the scalar mesons as anticipated by the quark model. In view of this result, we make some remarks on possible connections between the $^3P_0$ pair creation model, scalar mesons, and the $U_A(1)$ anomaly responsible for the large OZI violation which drives the η' mass.

DOI: 10.1103/PhysRevD.64.094507 PACS number(s): 12.38.Gc, 11.15.Pg, 12.38.Aw, 12.39.−x

I. BACKGROUND

The phenomena which led to the formulation of the Okubo-Zweig-Iizuka (OZI) rule [1,2] have had a definitive impact on our understanding of strong interactions. The fact that ''aces'' (i.e., quarks) led to a simple interpretation of the properties of the ϕ meson was clearly a very important clue for Zweig [1] since it was natural for the ϕ to be pure $s\bar{s}$ and for certain ϕ production cross sections to be small so long as ''hairpin graphs'' were dynamically suppressed (see Fig. 1).

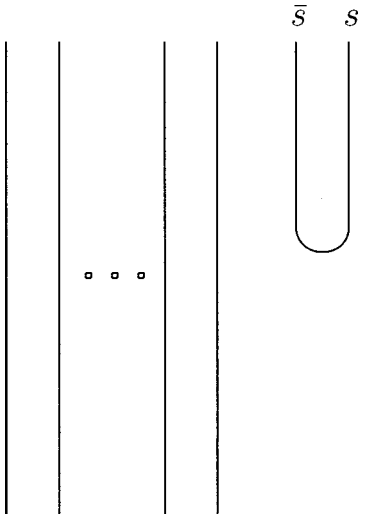

FIG. 1. A typical hairpin reaction, where the two lines–ellipsis–two lines on the left denote an arbitrary OZI-allowed process and an $s\bar{s}$ hairpin is shown for concreteness. Note that gluonic fields and closed $q\bar{q}$ loops are not represented since the external quark line topology is all that is relevant to the rule.

The dynamics behind the suppression of hairpin graphs in QCD has remained unexplained. The *phenomenology* of meson mixing angles in QCD-based quark models was described in the mid-1970s in a number of papers [3–5]. In such models, processes with the quark line topology of the double-hairpin graphs of Fig. 2(b) (but with arbitrary time orderings) modify the quark-antiquark transition amplitudes from the totally flavor diagonal form associated with the ''scattering'' quark line topology of Fig. 2(a), namely,

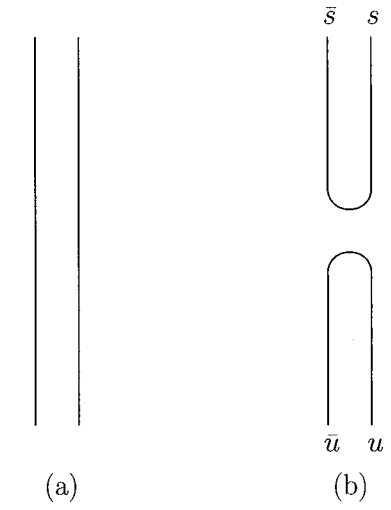

FIG. 2. Quark line diagrams associated with the OZI rule in meson nonets: (a) a normal OZI-conserving quark-antiquark ''scattering'' process, (b) a typical double-hairpin ''annihilation'' process leading to flavor mixing in meson wave functions. Since the OZI-violating reactions of Fig. 1 could occur through OZI-allowed meson emission followed by flavor mixing, these processes are the simplest manifestations of OZI violation. Note that gluonic fields and closed $q\bar{q}$ loops are not represented since the external quark line topology is all that is relevant to the rule.

$$\mathbf{T}=\begin{bmatrix} S & 0 & 0 & 0 \\ 0 & S & 0 & 0 \\ 0 & 0 & S & 0 \\ 0 & 0 & 0 & S \end{bmatrix} \tag{1}$$

[for illustrative purposes we have suppressed all space-time labels and specialized to the case of $SU(2)$ flavor where the matrix spans the basis $u\bar{d}$, $d\bar{u}$, $u\bar{u}$, $d\bar{d}$] by the addition of the annihilation amplitudes A:

$$\mathbf{\Delta T}=\begin{bmatrix} 0 & 0 & 0 & 0 \\ 0 & 0 & 0 & 0 \\ 0 & 0 & A & A \\ 0 & 0 & A & A \end{bmatrix}. \tag{2}$$

Using this framework [6], it was noted that the OZI mixing amplitude A characterizing Fig. 2(b) was of order 10 MeV in the established meson nonets, with the sole exception of the ground state pseudoscalar meson nonet, where A is an order of magnitude larger. These observations were consistent with the pattern one would expect for heavy quarkonia where the ground state pseudoscalar double hairpin is larger than the vector double hairpin by one factor of $(\alpha_s/\pi)^{-1}$, and orbitally excited state double hairpins are suppressed by having vanishing wave functions at $\vec{r}=0$. However, an explanation for this pattern in light quark systems was lacking.

The large size of the ground state pseudoscalar double hairpin is a manifestation of the "$U_A(1)$ problem" [7]: the equations of motion of QCD, taken naively, would imply that spontaneous chiral symmetry breaking leads to *nine* and not just eight Goldstone bosons [8], but the large mass of the η' seems to disqualify it from the role of the flavor singlet Goldstone boson. However, the $U_A(1)$ current is anomalous, and by the late 1970s it was understood through the study of instantons [9,10] that the anomaly leads to a nonconservation of the $U_A(1)$ charge and thereby to the evasion of Goldstone's theorem in the flavor singlet channel when chiral symmetry is spontaneously broken. The connection between the quark model picture of double hairpins and instantons was discussed by Witten [11], Veneziano [12], and others, who explored more generally the conflict between instantons and the large N_c expansion [13].

[The reader familiar with instanton lore may be puzzled by the connection between the annihilation amplitudes $A_{OZI}^{0^{-+}}$ of Eq. (2) in the pseudoscalar mesons and instanton-induced effects in the pseudoscalar mesons. The latter effects are associated with the 't Hooft interaction [10] which [in our illustrative $SU(2)$ flavor case] leads to $u\bar{u}\to d\bar{d}$ and $d\bar{d}\to u\bar{u}$ but *not* the diagonal entries in Eq. (2) for ΔT corresponding to $u\bar{u}\to u\bar{u}$ or $d\bar{d}\to d\bar{d}$ transitions. Recall, however, that the 't Hooft interaction also has $u\bar{d}\to u\bar{d}$ and $d\bar{u}\to d\bar{u}$ interactions, i.e., the S-like amplitudes of Eq. (1). Thus the instanton-induced interactions also admit the decomposition of Eqs. (1) and (2) with $S=-A$. We will elaborate upon this point below.

TABLE I. OZI-violating amplitudes in meson nonets. These amplitudes are defined to be the contribution of the $u\bar{u}\to d\bar{d}$ double hairpin to the nonet mass matrix.

Nonet	Empirical $A_{OZI}^{J^{PC}}$ (MeV)	Quark model loop contribution to $A_{OZI}^{J^{PC}}$ (MeV) [a]
0^{-+}	$+400\pm200$ [b]	- - -
1^{--}	$+7\pm1$	-2 ± 4
2^{++}	-22 ± 3	$+6\pm14$
1^{++}	$+11\pm15$	$+12\pm12$
0^{++}	see text	-450 ± 200 [b]
1^{+-}	-32 ± 12	-15 ± 7
3^{--}	-12 ± 4	$+4\pm7$
4^{++}	$+6\pm18$	$+16\pm7$

[a]The quoted "theoretical error" assigned here is the range quoted in Ref. [17] for meson loop processes from reasonable parameter variations.
[b]See Ref. [14].

The large N_c expansion is the only known field-theoretic basis for the general success of the valence quark model, Regge phenomenology, the observed narrowness of resonances, and the OZI rule. In particular, the OZI-violating meson mixing amplitudes of Fig. 2(b) are all of order $1/N_c$. Ironically, such a suppression of these amplitudes seems perfectly consistent with the effects in the pseudoscalar mesons, but not strong enough to account for the extremely small amplitudes seen in other nonets. See the second column of Table I.

The unexpected suppression of most OZI-violating amplitudes beyond a simple factor of $1/N_c$ is elevated from a dynamical puzzle to a paradox when the various time orderings of Fig. 2(b) are projected into a hadronic basis. In such a basis, flavor mixing could arise through an intermediate glueball, through an instantaneous interaction, or via a hadronic loop process in which Fig. 2(b) has the time ordering shown in Fig. 3. The paradox arises from the observation [15] that these OZI-violating hadronic loop processes can proceed by sequential *OZI-allowed* vertices with known and unsuppressed strengths. These hadronic loop diagrams may be associated with contributions to meson propagators arising from second order (real and virtual) decay processes, and as such are of order $(1/\sqrt{N_c})^2$, as expected. This factor of $1/N_c$ is also perfectly consistent with the observation that the *imaginary* parts of these propagators give the $1/N_c$-suppressed meson widths which are generally of order of *hundreds* of MeV. Nevertheless, OZI phenomenology requires that the $1/N_c$-suppressed *real* parts (from the full meson spectrum and not just the kinematically allowed part) be an order of magnitude smaller. Explicit model calculations substantiate the generic result that individual hadronic channels of the type depicted in Fig. 3 would indeed contribute hundreds of MeV to OZI-violating meson mixing. Thus even if the other possible sources of OZI violation (from the other time orderings) were dynamically suppressed, these hadronic loop diagrams would seem to spoil the OZI rule. This rule requires that $A_{OZI}\ll m_s-m_d$ so that the nonet and not the

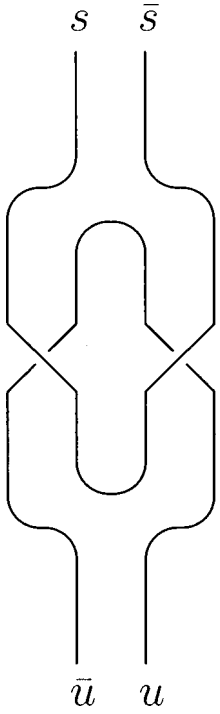

FIG. 3. Two sequential OZI-allowed processes can lead to the topology of Fig. 2(b).

$SU(3)$ limit is realized. Thus it is a necessary (but not sufficient) condition for the OZI rule that there be some conspiracy between hadronic loop processes which suppresses them below their expected $1/N_c$ strength [16].

II. A PROPOSED RESOLUTION

The authors of Ref. [17] proposed a resolution of this paradox. They examined the OZI-violating amplitudes A_{OZI} in non-pseudoscalar channels from the *complete* tower of hadronic loop processes to determine if ''miraculous'' cancellations between the hundred-MeV-scale real parts of individual channels could be responsible for the suppression of the sum over channels beyond a simple power of $1/N_c$. To make such a calculation one must have a complete model for meson trilinear vertices since; if such a conspiracy is to occur, it will have to be based on an underlying pattern of coupling *strengths* and *signs*. The nonrelativistic quark model is complete in this sense: using the standard $^3P_0$ pair creation operator for hadronic decays by flux tube breaking [18] and valence quark model wave functions, all trilinear vertices and their associated form factors are prescribed. Since the model is a nonrelativistic one, only the time ordering of Fig. 3 with a two meson intermediate state can be calculated in this way, but within this framework Ref. [17] shows that in general a ''miraculous'' cancellation between channels does indeed occur. This cancellation occurs between groups of intermediate meson states that might have been difficult to anticipate *a priori*. Consider the prototypical case of $\omega-\phi$ mixing where $\omega\rightarrow(AB)_L\rightarrow\phi$ with L the AB relative angular momentum. The intermediate states contributing to Fig. 3 are $(K\bar{K})_P$, $(K\bar{K}^*)_P$, $(K^*\bar{K}^*)_P$, $(K^*\bar{K}_0^*)_S$, $(K\bar{K}_{a_1})_S$, $(K\bar{K}_{a_1})_D$, $(K^*\bar{K}_{a_1})_S$, $(K^*\bar{K}_{a_1})_D$, $(K\bar{K}_{b_1})_S$, $(K\bar{K}_{b_1})_D$, $(K^*\bar{K}_{b_1})_S$, $(K^*\bar{K}_{b_1})_D$, $(K\bar{K}_2^*)_D$, $(K^*\bar{K}_2^*)_S$, $(K^*\bar{K}_2^*)_S$, ... where K and K^* are the ground state ($l=0$) pseudoscalar and vector mesons, and K_0^*, K_{a_1}, K_{b_1}, and K_2^* are the first excited state ($l=1$) strange mesons with $J^P=0^+,1^+,1^-$, and 2^+ which would be associated with the a_0, a_1, b_1, and a_2 octets in the $SU(3)$ limit. (Note that the ellipsis denotes more highly excited intermediate states, including ones in which *each* leg of the intermediate state is excited, and that charge conjugate intermediate states are implied.) As expected on the basis of the previously described arguments, a typical channel in this sum contributes of order 100 MeV to $A_{OZI}^{1^{--}}$. However, intermediate states with the same *total orbital angular momentum* but opposite values of $(-1)^L$ tend to cancel. Thus, for example, the $(l_A=0,l_B=0)_P$ channels with $L_{total}\equiv l_A+l_B+L=1$ all have the same sign, but they strongly cancel against the $(l_A=0,l_B=1)_S+(l_A=1,l_B=0)_S$ channels.

The calculation is formidable. With standard quark model parameters the form factors are quite hard and complete convergence is achieved only after summing of order 10 thousand channels, corresponding to $L_{total}\simeq 10$. With reasonable variations of standard parameters the contribution of an individual channel waxes and wanes, as does the speed of convergence. However, *the underlying mechanism of the cancellation is simple and very robust:* $A_{OZI}^{1^{--}}$ *is much smaller than its component pieces because of an approximate "spectator plus closure limit."* This limit is illustrated in Fig. 4, which shows the standard $^3P_0$ operator with $J^{PC}=0^{++}$ trying to create and then annihilate quark-antiquark pairs with $J^{PC}=1^{--}$. If a single two meson intermediate state is inserted into this diagram, it will project out pieces of this amplitude of order $1/N_c$ as expected, but if the original (final) $q\bar{q}$ pair does not distort the J^{PC} of the produced (annihilated) pair (the spectator approximation) a complete set of intermediate states with a common energy denominator (the closure approximation) *will give zero amplitude*. Reference [17] shows that deviations from this ''spectator plus closure limit'' are naturally small, leading to the observed order of magnitude suppression of the loop contribution to $A_{OZI}^{1^{--}}$ relative to $1/N_c$ expectations. See Table I. The interested reader is referred to Ref. [17] for a detailed explanation of the resiliency of this limit. This quark model solution to the ''second order paradox'' associated with the OZI rule also appears to justify the conspiracies between Regge trajectories required to explain the suppression of cross sections requiring ''exotic'' exchanges (e.g., those with isospin 2) [19]. Since ''exotic'' exchanges can occur by double Regge exchanges (analogous to the second order loop processes), only a conspiracy between exchanges (analogous to the conspiracy between loops) can give the observed suppression of such cross sections.

While the order of magnitude suppression of the loop contribution to $A_{OZI}^{1^{--}}$ is robust, the contribution of individual channels and the residue after the cancellations have occurred is model sensitive, so a prediction for the actual value of this amplitude cannot be made. This is not a great loss,

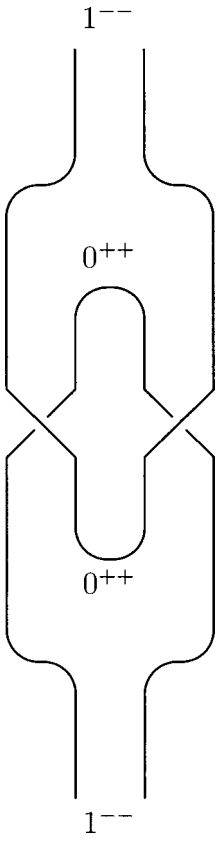

FIG. 4. A graphical representation of the ''spectator plus closure limit'': in this limit the 0^{++} pair creation operator cannot destroy or create a 1^{--} pair.

however, since the accuracy of the model is very suspect: its dynamics is nonrelativistic, and it has ignored the *Z*-graph time orderings of Fig. 3. More significantly, any such amplitude would need to be added to the unknown pure glue and instantaneous contributions to the $q\bar{q}\to q'\bar{q}'$ transition before being compared to experiment. Thus the important conclusion of Ref. [17] is the *qualitative* one that the ''second order paradox'' can be evaded.

Reference [17] confirms that A_{OZI} from meson loop diagrams is small in not only the vector mesons but in all other well-established nonets: those with $J^{PC}=2^{++},1^{++},1^{+-},3^{--}$, and 4^{++}. The key, of course, is that the nonet J^{PC} must differ from that of the $^3P_0$ pair creation operator [20]. From this simple requirement follows a rather spectacular prediction: *OZI violation should be very strong in the scalar meson nonet.*

The scalar mesons, and especially the isoscalar scalar mesons which would display the effects of OZI violation, have been notoriously difficult to understand experimentally. Over the last 30 years the mass of the lightest isoscalar scalar meson quoted by the Particle Data Group has varied between 400 and 1400 MeV, while the quoted width has varied between and 100 and 1000 MeV. (We have removed the $f_0(980)$ from this compilation under the presumption that it is a $K\bar{K}$ molecule, or this spread of values would be even wider.) The experimental status of the scalar meson nonet becomes even more obscure when one recalls that the lightest glueball is expected to have $J^{PC}=0^{++}$ and a mass around 1.5 GeV. One can only say with confidence that the experimental situation does not exclude that $A_{OZI}^{0^{++}}$ is large.

Fortunately, there is an alternative to checking this prediction of the quark model mechanism against experiment. We can check it against calculations from lattice QCD.

III. OZI ON THE LATTICE

A. OZI violation in the quenched approximation

Matrix elements of the type $\langle 0|T[\bar{q}'(y)\Gamma^{J^{PC}}q'(y)\bar{q}(x)\Gamma^{J^{PC}}q(x)]|0\rangle$, where $\Gamma^{J^{PC}}$ carries space-time indices that determine the J^{PC} of the propagator being studied and $q'\neq q$, describe OZI violation in mesons. In leading order in $1/N_c$, such processes can proceed through diagrams of the type depicted in Fig. 2(b) (of which Fig. 3 is the particular time-ordering relevant to the hadronic loop diagrams), i.e., they receive leading contributions in the quenched approximation in which internal quark-antiquark loops are ignored. (Of course the *accuracy* of the quenched approximation can be questioned, but this is irrelevant to the main points of this paper, including checking a prediction of the quark model in which internal quark loops are also neglected.)

In the absence of OZI violation, the ω-like $(1/\sqrt{2})(u\bar{u}+d\bar{d})$ and ϕ-like $s\bar{s}$ sectors are segregated and each develops its own tower of meson excited states of each allowed J^{PC}. If the OZI-violating amplitudes $A_{OZI}^{J^{PC}}$ in that channel are small, then in leading order they simply shift the masses of each state by $\sim A_{OZI}^{J^{PC}}$ and create $\omega-\phi$-like mixing with a mixing angle $\sim A_{OZI}^{J^{PC}}/\Delta m$ where Δm is the unperturbed mass difference between the ω- and ϕ-like states being mixed. In such circumstances the empirical value of $A_{OZI}^{J^{PC}}$ may be extracted from either the $\omega-\rho$-like mass difference or the $\omega-\phi$-like mixing angle and compared directly with the quenched lattice amplitudes since the latter may be construed as correctly representing OZI violation in the quenched approximation in lowest order perturbation theory in $A_{OZI}^{J^{PC}}$.

If $A_{OZI}^{J^{PC}}$ is strong, as in the pseudoscalar channel, the situation is more complicated. In such circumstances two new effects come into play: the masses of ω- and ϕ-like states can be shifted strongly, so that their mixing angle may not be determined by their unperturbed mass difference, and treating the mixed propagator from $q\bar{q}\to q'\bar{q}'$ in lowest order in $A_{OZI}^{J^{PC}}$ may not be valid. The former effect is straightforward, but the latter can be complex. For example, a higher order treatment of $A_{OZI}^{J^{PC}}$ appears to be inconsistent with the quenched approximation, as shown in Fig. 5. However, the process depicted in Fig. 5 is one of a series of processes with internal quark loops that arise from repeated iteration of the quenched amplitude. Their effect and that of the diagonal mass shifts is to create a propagator *matrix* with entries corresponding to the quenched approximation; when diagonalized perturbatively this matrix gives the masses and mixing angles for weak OZI violation, but for strong OZI violation it

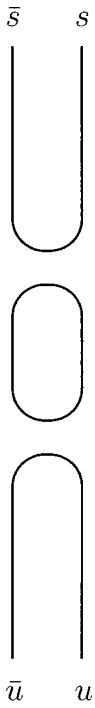

FIG. 5. A contribution to OZI-violating meson mixing which is superficially inconsistent with the quenched approximation.

may be diagonalized exactly, thereby summing the series of sequential applications of $A_{OZI}^{J^{PC}}$. Another closely related possible complication is that a large $A_{OZI}^{J^{PC}}$ can create strong mixing with the glueball sector, requiring that the propagator matrix be enlarged yet further.

For the pseudoscalar mesons, the preceeding discussion of the effects of a large A_{OZI} are particularly significant. In the chiral limit with $A_{OZI}^{0^{-+}}=0$, the $U_A(1)$ meson—the η'—is also massless. As a result, the quenched OZI-violating amplitude of Fig. 3 will give $A_{OZI}^{0^{-+}}$ sandwiched between two massless propagators, i.e., it will give an η' propagator that looks nothing like that of a massive, $SU(3)$-flavor-mixed η'. In this case, to even *qualitatively* relate the quenched amplitudes to nature one must extract $A_{OZI}^{0^{-+}}$ from them and add these amplitudes to the propagator *matrix* [the broken $SU(3)$ analog of Eq. (1)] which one diagonalizes exactly. The resulting full propagator will have a massive $SU(3)$-flavor-mixed η' which sums the single particle effects of $A_{OZI}^{0^{-+}}$ to all orders. Further numerical support for this interpretation of the quenched pseudoscalar double hairpin comes from the shape of the double-hairpin propagator as a function of Euclidean time. As discussed below (see also Ref. [22]), this time dependence can be fit very well to the functional form $(1+m_\pi t)\exp(-m_\pi t)$ expected from a mass insertion vertex surrounded by two propagators of mass m_π.

B. Methods

The ability to study the double-hairpin diagrams relevant to the OZI rule has been greatly improved by two recent developments in lattice QCD methodology. The global source technique (which we refer to as the ''allsource'' method) was introduced several years ago for the purpose of studying the η' mass and the $U_A(1)$ anomaly [21]. In this method, the quark propagator is calculated from a sum of identical unit color-spin sources located at all space-time points on the lattice. If this allsource propagator is contracted over color indices at a *given* site, the result is a gauge invariant term corresponding to a closed quark loop originating from that site, plus a very large number of gauge-dependent open loops. The latter terms tend to cancel due to their random phases, allowing a determination of closed loop averages and loop-loop correlators (double hairpins). The other recently developed technique which has greatly improved the accuracy of the results for both double-hairpin calculations and for other chiral studies with Wilson-Dirac fermions is the modified quenched approximation (MQA) [22], which provides a practical resolution of the exceptional configuration problem that has long plagued such calculations. This method identifies the source of the exceptional configuration problem as the presence, in some gauge configurations, of exactly real eigenmodes which are displaced into the physical mass region by the artificial chiral symmetry breaking associated with the lattice Wilson-Dirac operator. By systematically identifying these real eigenmodes and calculating their contribution to the quark propagators, the corresponding propagator poles can be extracted and moved to zero quark mass (where they belong). This MQA procedure has been applied to both the allsource propagators for double-hairpin calculations as well as to valence quark propagators. The resulting MQA-improved propagators have recently been used in an extensive study of quenched chiral logs and their relation to the η' mass and the $U_A(1)$ anomaly [24]. As a part of this study, the size and time dependence of the pseudoscalar η' double-hairpin diagram was calculated, using the allsource method. Since the pole-shifting procedure has already been applied to the quark propagators, it requires very little additional effort to investigate the vector, axial-vector, and scalar double-hairpins which determine the spin-parity pattern of OZI mixing. The results we present here are from a set of 300 quenched gauge configurations on a $12^3\times 24$ lattice at $\beta=5.7$. In the study of Refs. [22,24], both naive Wilson and clover improved quark actions were studied. It was found that, at $\beta=5.7$ with the Wilson action, substantial lattice spacing effects suppressed the pseudoscalar double hairpin, giving a smaller than expected value of $\mathbf{A}_{OZI}^{0^{-+}}=(0.27\ \text{GeV})^2$ for the double-hairpin contribution to the η' mass versus the value $(0.49\ \text{GeV})^2$ extracted from weak-$SU(3)$-breaking mass formulas [14]. A much more satisfactory result is obtained from the clover improved quark action. With a clover coefficient $C_{sw}=1.57$, the pseudoscalar double hairpin gives $\mathbf{A}_{OZI}^{0^{-+}}=(0.41\ \text{GeV})^2$. For the calculation of OZI-violating amplitudes, we will therefore use the clover improved quark action only; we also use the physical charmonium $1S$-$1P$ splitting to set the scale ($a^{-1}=1.18$ GeV) for $\beta=5.7$ when we quote lattice results in physical units [25].

C. Results

Using the method described in the previous section, we have calculated the double-hairpin contribution to matrix elements of the form

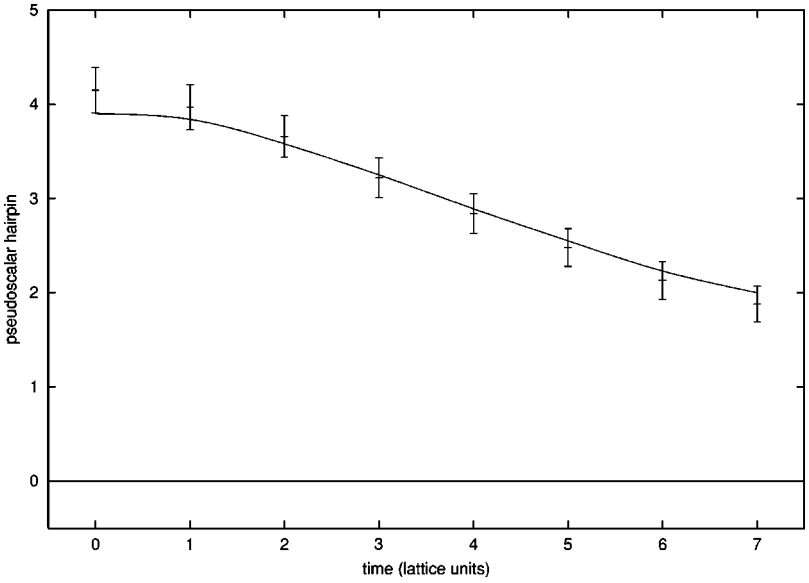

FIG. 6. The pseudoscalar double-hairpin correlator for $\kappa = .1427$. Note that this amplitude had an overall negative sign, corresponding to a positive pseudoscalar mass shift. The fit shown is a 1-state fit of the form Eq. (6).

$$\langle \overline{q}'(y)\Gamma^i q'(y)\overline{q}(x)\Gamma^i q(x)\rangle \tag{3}$$

with Hermitian operators generated by the choices $\Gamma^i = i\gamma_5$ (pseudoscalar), $\Gamma^i = \gamma^\mu$, $\mu = 1,2,3$ (vector), $\Gamma^i = \gamma^\mu\gamma_5$, $\mu = 1,2,3$ (axial vector), and $\Gamma^i = 1$ (scalar) (the antisymmetric tensor $\sigma^{\mu\nu}$ does not explore new states: it also has axial vector quantum numbers). As in standard hadron spectroscopy, we Fourier transform the space-time propagator over 3-dimensional time slices at zero 3-momentum and study its time dependence. A particular advantage of the allsource method is that the Fourier transforms can be performed over both ends of the meson propagator, unlike the usual case of a fixed local source where only one end can be transformed. This provides an improvement in statistics which is quite important for the success of the method. For the scalar double-hairpin matrix element, the expectation value of a single scalar loop is nonzero, and so a constant proportional to $\langle 0|\overline{q}q|0\rangle^2$ must be subtracted from the above matrix element to get the true correlator.

Even without any detailed analysis, the overall empirical OZI pattern of Table I is strikingly confirmed by the lattice results. This is easily seen from the size of the various double-hairpin correlators. In Figs. 6–9, we have plotted the double-hairpin correlators for the pseudoscalar, vector, axial vector, and scalar sources. All plots have the same scale for comparison. The calculations have been done for seven different choices of quark mass. The data shown in the figures are from one of the lightest quark masses ($\kappa = .1427$), for which the pion mass is about 300 MeV ($m_\pi a = 0.266 \pm 0.004$). The results quoted in Table II are chirally extrapolated to the physical pion mass. By far the largest and longest-range correlator is the pseudoscalar correlator of Fig. 6. This is expected for two reasons: the anomaly introduces a large double-hairpin vertex responsible for the large η' mass, and, as explained above, in the quenched approximation the external $\overline{q}q$ meson propagators on either side of the double-hairpin vertex are light Goldstone bosons. The results for the pseudoscalar case have been studied in detail in Ref. [24].

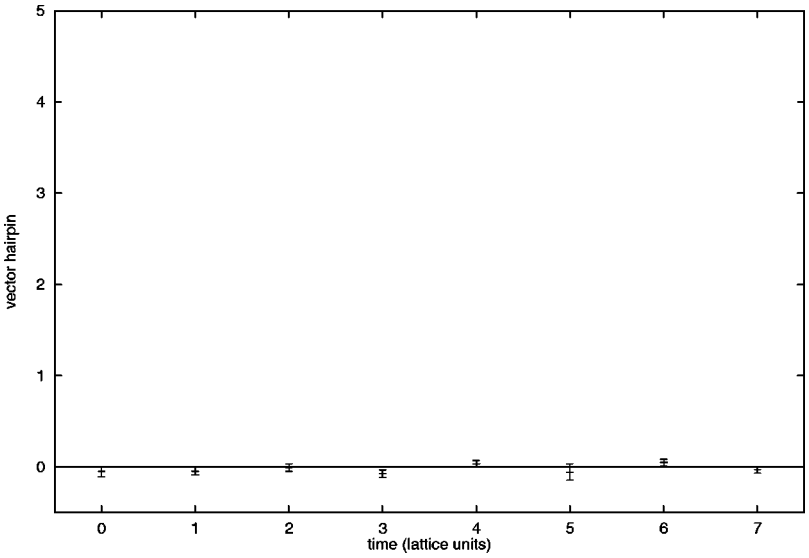

FIG. 7. The vector double-hairpin correlator for $\kappa = .1427$.

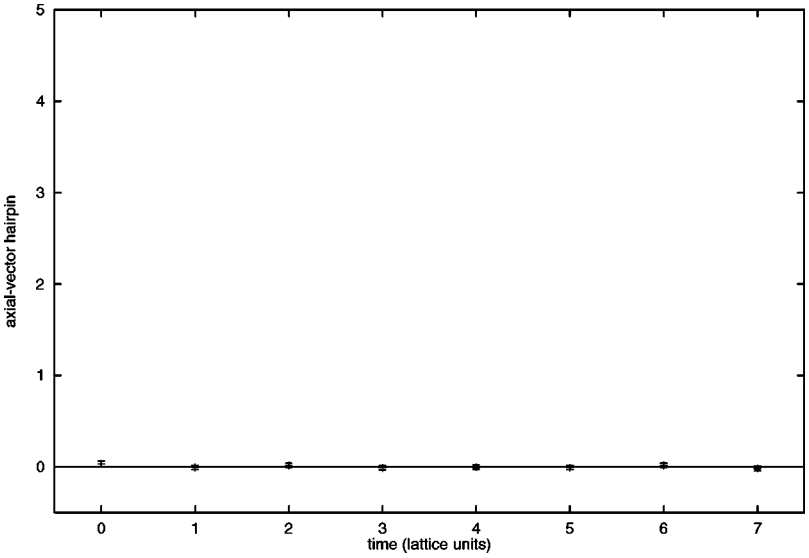

FIG. 8. The axial vector double-hairpin correlator for $\kappa = .1427$.

Compared to the very strong pseudoscalar double hairpin, the vector and axial vector double hairpins of Figs. 7 and 8 are dramatically suppressed, consistent with the empirical observations described in Sec. I. Since quenched lattice QCD gives reasonable values for the three-point functions associated with the meson virtual loop processes depicted in Fig. 3, these results provide not only a first derivation of the OZI rule from QCD, but also a dramatic example of the evasion in QCD of the ''second order paradox'' described in Sec. I and a confirmation of the fact that in a complete calculation a conspiracy of the type described in Sec. II must occur. [Of course the results reported here include not only the meson loop contributions but also the other time orderings of the double-hairpin graphs of Fig. 2(b).] We in fact see no significant signals in the vector and axial vector channels and so report in Table II only one standard deviation upper bounds.

As described in Sec. II and illustrated in Fig. 4, if the conspiratorial cancellation among meson loops is associated with $^3P_0$ pair creation, one would expect $A_{OZI}^{0^{++}}$ to be very large. Figure 9 shows this behavior: after taking into account the heavier mass of the scalar meson (about 1.25 in lattice units [26]), we find that the scalar OZI amplitude is comparable in size to the pseudoscalar amplitude but of the opposite sign (see Table II). A full amplitude A_{OZI} in general has glueball, instantaneous, and loop contributions, and in a given amplitude, any or all of these components might be important. (Recall, for example, that while the loop contribution to $A_{OZI}^{0^{-+}}$ is believed to be small [20], the full $A_{OZI}^{0^{-+}}$ is large.) That the measured $A_{OZI}^{0^{++}}$ is actually consistent in sign and magnitude with the hadronic loop contribution predicted by the quark model has interesting implications which we will discuss below. A large and negative $A_{OZI}^{0^{++}}$ has been previously reported in Ref. [27].

To obtain the quantitative results for the OZI mixing amplitudes quoted in Table II, we carried out an analysis similar to that used to obtain the η' mass from the pseudoscalar double hairpin [22,24]. For that case, the time dependence of

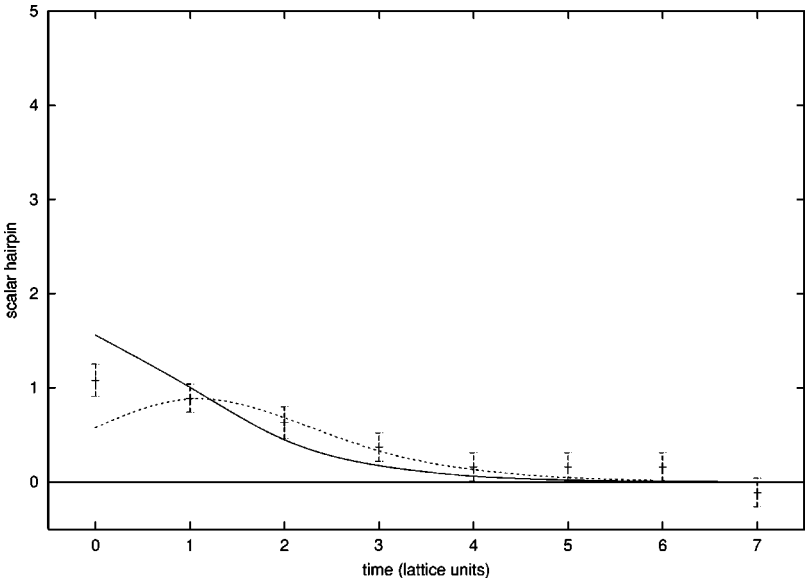

FIG. 9. The scalar double-hairpin correlator for $\kappa = .1427$. The solid and dashed curves are a 1-state fit and a 2-state fit, respectively.

TABLE II. Quenched lattice OZI-violating amplitudes.

Nonet	$\mathbf{A}_{OZI}^{J^{PC}}$ (MeV)^2	$A_{OZI}^{J^{PC}}$ (MeV)[a]
0^{-+}	$+(407\pm 11)^2$	$\simeq +290$
1^{--}	$<(220)^2$	<30
1^{++}	$<(380)^2$	<60
0^{++}	$-(1350\pm 90\pm 320)^2$	$\simeq -520$

[a]For the conversion from $\mathbf{A}_{OZI}^{J^{PC}}$ extracted from the lattice via Eq. (6) to $A_{OZI}^{J^{PC}}$ for comparison to the amplitudes quoted in Table I based on mass matrices, see Ref. [14]. For the 0^{++} state, the first error shown in column 2 is statistical only. The second is the error associated with excited state contamination. See discussion at the end of Sec. III.

the pseudoscalar double-hairpin correlator corresponding to Fig. 2(b) was found to be quite well described by a ''double-pole'' form consisting of a p^2-independent double-hairpin insertion between a pair of meson propagators (see also Ref. [14]). Thus we assume that

$$\tilde{\Delta}_{dh}^{i}(p) = -f_i \frac{1}{p^2+m_i^2} \mathbf{A}_{OZI}^{i} \frac{1}{p^2+m_i^2} f_i, \tag{4}$$

where f_i is the vacuum-to-one-particle matrix element

$$f_i = \langle 0|\bar{q}\Gamma^i q|M^i(p)\rangle, \tag{5}$$

m^i is the meson with the quantum numbers 0^{-+}, 1^{--}, 1^{++}, and 0^{++} of the four operators $\bar{q}\Gamma^i q$ defined at the beginning of this section, and $\mathbf{A}_{OZI}$ is the (mass)^2 version of the A_{OZI} defined previously [14] (called m_0^2 in Refs. [22,24]). This gives a time-dependent double-hairpin correlator at zero 3-momentum of the form

$$\Delta_{dh}(\mathbf{p}=0;t) = -\frac{f_i^2 \mathbf{A}_{OZI}^{i}}{4m_i^3}(1+m_i t)e^{-m_i t} + [t \to (Na-t)] \tag{6}$$

to be compared to the usual valence quark (e.g., isovector) correlator corresponding to Fig. 2(a)

$$\tilde{\Delta}_{v}(p) = f_i \frac{1}{p^2+m_i^2} f_i \tag{7}$$

which gives

$$\Delta_{v}(\mathbf{p}=0;t) = \frac{f_i^2}{2m_i} e^{-m_i t} + [t \to (Na-t)]. \tag{8}$$

[The relative sign of Eqs. (6) and (8) is tricky; with our convention a positive $\mathbf{A}_{OZI}$ makes a positive contribution to the (mass)^2 of a state.]

As described qualitatively above, for each channel i we independently determined m_i and f_i from a fit of Eq. (8) to the isovector (connected) correlator corresponding to Fig. 2(a). The resulting m_i and f_i are consistent at the level expected for a quenched calculation with what is known experimentally about m_π, m_ρ, m_{a_1}, and m_{a_0}, and about f_π, f_ρ, and f_{a_1} [26]. With these parameters determined, Eq. (6) allows a one parameter ($\mathbf{A}_{OZI}^{i}$) fit to the data of Figs. 6–9. These results, along with similar results for the other κ values, give the chirally extrapolated results shown in Table III. The second error quoted on the 0^{++} amplitude is the estimated systematic error associated with excited state contributions to the correlator, as discussed at the end of this section.

The estimates of ground state parameters in Table II are subject to several standard sources of systematic error. These include finite volume and finite lattice-spacing effects, effects of quenching, and uncertainties due to excited-state meson contributions to the hairpin correlators. Investigation of finite volume and lattice spacing errors will require more extensive Monte Carlo calculations on different size lattices. Experience with other hadronic calculations at these lattice parameters suggests that finite volume errors should be $<10\%$. (The spatial length of the lattice is approximately 2.0 fm.) Lattice spacing errors are potentially more serious, We would expect them to be at the $<20\%$ level based on other meson masses and decay constants at this value of β. Some caution may be warranted, however, as more serious scaling violations of up to 50% arise in the glueball sector. We do not expect lattice spacing effects to alter the essential conclusions of our study, but it is clearly important to repeat these calculations at larger values of β. Within the context of

TABLE III. Fits to the scalar hairpin correlator with and without excited state terms included. Columns 2 through 4 are the parameters of a 2-state fit with masses held fixed at values determined from valence propagator fits as discussed in the text. Columns 5 and 6 give the coefficient and χ^2/dof for a single-state fit.

κ	$A_{0^{++}}$(2 state)	$A^*_{0^{++}}$(2 state)	χ^2/dof	$A_{0^{++}}$(1 state)	χ^2/dof
.1410	1.25(47)	−.71(69)	1.4/4	.85(13)	2.4/5
.1415	1.37(44)	−.82(61)	1.9/4	.93(12)	3.6/5
.1420	1.51(47)	−.87(62)	0.8/4	.98(12)	2.8/5
.1423	1.68(52)	−.97(64)	0.6/4	1.02(13)	2.8/5
.1425	1.96(57)	−1.15(69)	1.9/4	1.17(14)	4.6/5
.1427	2.43(67)	−1.52(79)	1.6/4	1.30(17)	5.3/5
.1428	2.11(53)	−1.47(62)	1.9/4	1.28(17)	7.6/5

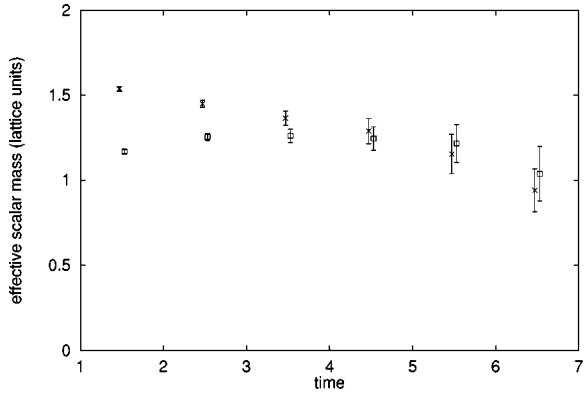

FIG. 10. Effective mass plot for the scalar valence propagator.

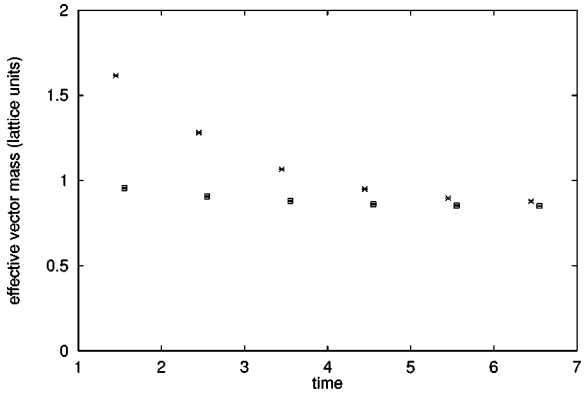

FIG. 12. Effective mass plot for the vector valence propagator.

the quenched approximation, perhaps the largest of the systematic errors associated with our $\mathbf{A}^i_{OZI}$ determination may be the assumption that each channel is dominated by a single lowest state [14].

Undoubtedly as better statistics and finer lattices become available, one will be able to perform multichannel fits which will eliminate excited-state contributions in each channel. Some indication of the level of excited state contamination can be obtained from effective mass plots of the valence (connected) propagators in each spin-parity channel. In Figs. 10–13, we show the effective mass plots for scalar, pseudoscalar, vector, and axial-vector channels, respectively. In each plot, the upper points represent the effective mass using local sources, while the lower points are the effective mass using exponentially smeared sources in Coulomb gauge, with a smearing function $\propto \exp[-0.5t]$ in lattice units.

To obtain some estimate of the error due to excited states in the scalar double-hairpin amplitude, we have utilized the results of a recent study of the scalar valence (isovector) correlator [23]. By studying local and smeared correlators, it was estimated that, for the heaviest quark masses studied here ($\kappa = .1410$), the ground state and excited state scalar mesons have masses

$$m_{a_0} = 1.25(2), \quad m_{a_0^*} = 1.9(1) \tag{9}$$

in lattice units. With these masses fixed, we can perform correlated fits to a formula which includes both ground-state and excited-state terms of the form (6). (Note: It is essential for the stability of the hairpin fits to use the additional information from the valence propagator analysis to fix the masses.) The dependence of m_{a_0} and $m_{a_0^*}$ on quark mass was found in Ref. [23] to be fairly mild, changing by less than 10% over the entire range of quark masses studied. We have neglected this dependence and used the estimate (9) for the hairpin correlator fits at all mass values. The results for the seven quark masses studied are shown in Table III. The second and third columns give the coefficients of the ground-state and excited-state terms (in lattice units) for a 2-state fit over timeslices 1 through 6. The correlated χ^2/dof is shown in column 3. We also give in Table III the scalar hairpin coefficient and χ^2/dof extracted from a 1-state fit including only the ground state is shown in the last two columns. We see that in general the excited state coefficient is negative and the inclusion of excited states increases somewhat the estimate of the ground-state coefficient, while enlarging the error by more than a factor of 3. This provides us with an estimate of the systematic error associated with excited states, which is included as the second error on the chirally extrapolated 0^{++} OZI amplitude in Table II. The central value quoted for the 0^{++} amplitude in Table II is obtained from the 1-state fits in Table III, with the excited state error estimated from the 2-state fit. (The relevant fits for $\kappa = .1427$ are shown in Fig. 9.) The conclusion that $A^{0^{++}}_{OZI}$ is large is even stronger if the central value is extracted from

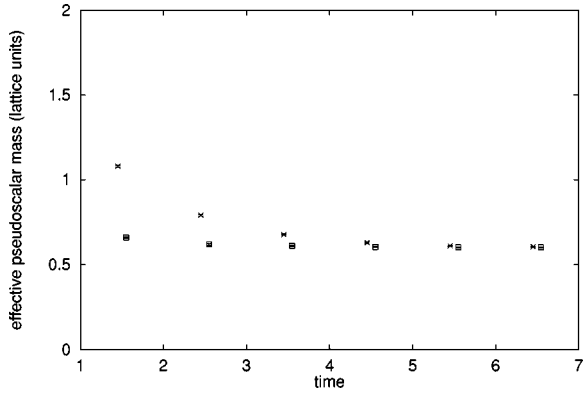

FIG. 11. Effective mass plot for the pseudoscalar valence propagator.

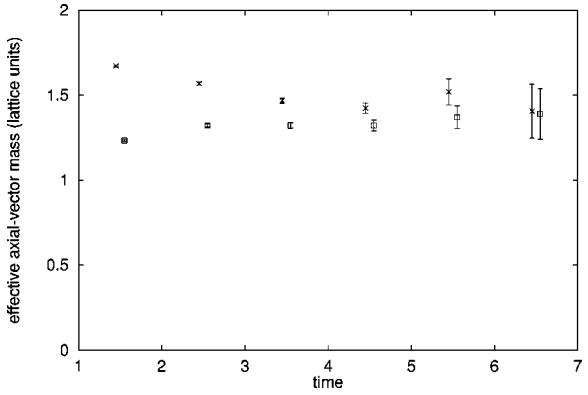

FIG. 13. Effective mass plot for the axial-vector valence propagator.

the 2-state fit. To compare results to nature, one will also have to go beyond the quenched approximation which experience suggests can only be expected to be accurate at the 20% level. However, as noted earlier, quenched information can be used to examine the viability of models, since they can typically make predictions for quenched observables, and this is probably the most important immediate use of our results. We will elaborate on this remark in the next two sections.

IV. CONCLUSIONS

The most straightforward conclusions of this work are that QCD can explain the OZI rule in channels where it is observed and that, although the quantitative estimate of $A_{OZI}^{0^{++}}$ has large systmatic uncertainties, it is reasonable to conclude that it is large and negative [27]. This is consistent with the quark model's explanation of the dynamical suppression of the typical scale of hadron-loop-induced OZI violation below $1/N_c$ expectations, and in so doing provides further evidence for the standard $^3P_0$ pair creation amplitude, since this is the critical feature which produces this result.

While the precise consequences are unclear, the implications for phenomenology are serious. With $A_{OZI}^{0^{++}}$ large, the lightest scalar meson nonet (the $1P$ states) will be close to the $SU(3)$ limit. We may therefore expect an octet of scalar mesons in the 1400 MeV range with the other $1P$ states while the nearly singlet scalar state will be substantially lower in mass. Thus the usual assumption of phenomenological analyses that this region will contain the unmixed nonet of $1P$ states and the scalar glueball is incorrect. For example, this region might well contain the isoscalar state of the $2P$ nonet. In addition, since $A_{OZI}^{0^{++}}$ is comparable to the $1P$-$2P$ splitting, there is no reason to assume that either the $1P$ or $2P$ singlet's properties can be related by nonet symmetry to those of its octet. The net effect is that the definitive extraction of the glueball state from the scalar meson spectrum may be quite difficult.

Given the importance of this task, it is certainly worthwhile to study the scalar mesons more carefully in the light of this result [28]. On the lattice it might be possible to obtain the matrix of OZI-violating amplitudes connecting the ω-like and ϕ-like $1P$ and $2P$ states; in models the low-lying scalar meson spectrum can be studied, including the effects of a strong annihilation channel.

Perhaps most critical is to use quenched lattice calculations of the mixed propagators from quarkonia to glueballs [28] to help resolve the scalar meson OZI violation reported here into the contributions of $q\bar{q}'q'\bar{q}$ intermediate states, purely gluonic intermediate states associated with ''true double-hairpin'' graphs, and instantaneous contributions. Ultimately, quenched lattice calculations of three-point functions could directly check the predicted negative loop contributions to $A_{OZI}^{0^{++}}$ by measuring the vertex functions which are the ''raw ingredients'' of the quark model calculation. In particular, in other than the 0^{++} channel, one should see the required magnitudes and *opposite signs* of the virtual *P*-wave decays to two $l=0$ mesons and the *S*-wave decays to one $l=1$ and one $l=0$ meson required to build up the near cancellation that is at the heart of the quark model mechanism. In contrast, for 0^{++} mesons these channels should have the same sign.

V. DISCUSSION

The results described here clearly have serious implications for the spectroscopy of 0^{++} states, and define the series of investigations described above required to clarify the physics behind $A_{OZI}^{0^{++}}$. Such investigations are not only important for their impact on phenomenology, however. They are also important because they address other more fundamental questions raised long ago by Witten [11], on the apparent conflict between the instanton solution of the η' mass [i.e., $U_A(1)$] problem and the large N_c limit. The quark model mechanism for the loop contributions to $A_{OZI}^{0^{++}}$ is based on large N_c. While our discussion of the $^3P_0$ model has focused on its prescription for the quantum numbers of the created $q\bar{q}$ pair, it is also an essential ingredient of the model that this pair creates $(q\bar{q}')+(q'\bar{q})$ and not $(q\bar{q})+(q'\bar{q}')$ mesons, i.e., that it respects the OZI rule at tree level. The physical picture behind this feature of the model is that pair creation (at order $1/N_c$) occurs by the breaking of the color flux tube connecting q and $\bar{q}$. More generally, as mentioned above, this limit provides the only known field-theoretic basis for the success of not only the valence quark model, but also of Regge phenomenology, the narrow resonance approximation, and many of the systematics of hadronic spectra and matrix elements [13,29–31]. In contrast, it is widely believed that the $U_A(1)$ problem is solved through instanton contributions to the axial anomaly. However, as emphasized by Witten, instantons vanish like e^{-N_c} and so do not appear in the large N_c expansion. ''Insofar as [instantons play] a significant role in the strong interactions, the large N_c expansion must be bad. It is necessary to choose between the two.'' [32] Note that these arguments draw an important distinction between semiclassically calculated instanton effects, which vanish like e^{-N_c}, and more general topological gauge fluctuations, which *can* contribute at order $1/N_c$ to $m_{\eta'}$. The real issue is not whether there are large fluctuations of $F\tilde{F}$ in the QCD vacuum, but whether these fluctuations arise as local semiclassical lumps with quantized winding numbers or simply as a result of the generically large gauge fluctuations of a confining vacuum.

To place this conflict in context, recall Eqs. (1) and (2). From Sec. III it is apparent that the amplitude for any of N_f massless $q\bar{q}$ pairs to annihilate to any other pair is the same, i.e., that ΔT does indeed have the form of the $N_f=2$ matrix shown in Eq. (2). As explained earlier, this is consistent with the 't Hooft instanton interaction since the ''scattering'' amplitude S in Eq. (1) contains a contribution $-A$ from instantons. Thus to leading order in A the decomposition of Eqs. (1) and (2) is general and the analyses of OZI violation in Refs. [3–5]— including that in the pseudoscalar sector—are valid. It follows that from a purely phenomenological per-

spective it is irrelevant whether or not there is an instanton contribution to hadronic physics: a phenomenology with $A_{OZI}^{0^{-+}} \neq 0$ is ''legal'' in any case, since the anomaly allows a resolution of the $U_A(1)$ problem with [9,10] or without [11,12] instantons. What remains unclear is the physics behind the annihilation amplitudes. Since a lattice simulation sums over all paths, it contains the instantons as tunnelling events between classical vacua, but the Feynman diagrams of QCD, which represent the quantum corrections around these vacua, are incapable of representing instanton physics. Thus if instantons are important in QCD, Feynman diagrams would have to be supplemented by effective interactions (the 't Hooft interaction). As noted by Witten [11], the foremost victim of the failure of Feynman diagrams implied if instantons are important would be the large N_c expansion, since it assumes that all-orders properties of the QCD Feynman diagrammatic expansion are properties of QCD.

We have demonstrated the feasibility of obtaining a lattice determination of the scalar OZI amplitude, adding one more item to a growing and closely linked set of issues where the physics of instantons and the physics of large N_c confront each other. Assuming that confinement and the Nambu-Goldstone mechanism [8] are properties of the all-orders Feynman diagrammatic expansion of QCD, the large N_c expansion provides a consistent framework embracing all strong interaction phenomena. Among these phenomena are the hadron spectrum for all flavors of hadrons (including the $1/N_c$-suppressed hadronic widths which seem to be critical to $A_{OZI}^{0^{++}}$), the OZI rule (now including $A_{OZI}^{0^{++}}$), and the $q\bar{q}$ condensate. As Witten argued long ago [11], given the $U_A(1)$ anomaly and confinement, the large N_c limit is also capable of explaining the η' mass at order $1/N_c$ *without* instantons.

While its limited range of applicability makes it somewhat less attractive for phenomenology (instantons offer a competing explanation only for the properties of the lightest $SU(3)_f$ hadrons),the instanton picture [33] has received strong support from recent lattice results [34]. Measurements of the topological charge [11] of ''cooled'' gauge configurations show that in such circumstances this charge is quantized and localized as expected for instantons. Moreover, the near-zero modes of the Dirac operator associated with the solution of the $U_A(1)$ problem and the $q\bar{q}$ condensate are also localized and in ''cooled'' configurations can be associated with these same instantons. The lattice results on these and other hadronic properties are consistent with the instanton liquid model [33].

Since, as argued by Witten, confinement can replace instantons as the source of the $U_A(1)$ anomaly and since confinement can also produce a space-time localization of the origin of the η' mass and of the $q\bar{q}$ condensate, in our view the true origin of these effects remains unsettled. Further investigation of the type initiated in this paper may help to resolve this situation since for $A_{OZI}^{0^{++}}$ the two competing pictures lead to mechanisms that are very distinct. Flux-tube-breaking pair creation, a prototypical large N_c phenomenon, led to the prediction that the hadron loop contribution to $A_{OZI}^{0^{++}}$ is large and negative as found here. Moreover, as stated in the beginning of this paper, quark models, with their confined constituent quarks, naturally generate a large positive $A_{OZI}^{0^{-+}}$ [35]. In this case the loop contribution should be typically small [20], and the large positive quark model amplitude is associated with an instantaneous interaction. Instantons, through the instantaneous 't Hooft interaction, would lead to a superficially similar pattern of OZI violation: a large positive $A_{OZI}^{0^{-+}}$ and a large negative $A_{OZI}^{0^{++}}$. However, the origins of the large negative $A_{OZI}^{0^{++}}$ are very different in the two cases: the instanton $A_{OZI}^{0^{++}}$ is associated with an instantaneous contribution while the quark model result arises from the contributions of two-meson intermediate states.

While the numerical coincidence of the A_{OZI}^{++} calculated here on the lattice and the A_{OZI}^{++} calculated in the quark model from meson loop diagrams might suggest that the instanton contribution to this amplitude is small, both calculations are too primitive to support such an important conclusion. Further studies of lattice spacing errors, finite volume effects, and excited state errors will be required to have confidence in the quantitative results.

Even having done such a calculation to satisfy oneself that an accurate value of A_{OZI}^{++} has been measured, to apply the result to the instanton–large-N_c controversy will require carrying out some of the additional work described in Sec. IV. In particular, to go beyond the circumstantial evidence provided by the quark model that A_{OZI}^{++} arises from meson loops, it will be necessary to use the techniques described there (or related ones) to break the lattice amplitude down into its component parts, thereby allowing one to see if the lattice result is indeed dominated by meson loop diagrams. We believe that through such studies, the conflict between large N_c and instanton physics can be resolved.

ACKNOWLEDGMENTS

We are grateful to Stephen Sharpe and Thomas Schaefer and to Chris Michael for alerting us to a serious sign error in the first version of this paper and to important references that had escaped our attention. This work was supported by DOE contract DE-AC05-84ER40150 under which the Southeastern Universities Research Association (SURA) operates the Thomas Jefferson National Accelerator Facility. The work of H.B. Thacker was supported in part by the Department of Energy under grant DE-FG02-97ER41027.

[1] G. Zweig, CERN Report No. 8419 TH 412, 1964; reprinted in *Developments in the Quark Theory of Hadrons*, edited by D. B. Lichtenberg and S. P. Rosen (Hadronic Press, Massachusetts, 1980). The history of the discovery of the quark model (or ''aces'') as seen by Zweig is related in ''Baryon 1980,'' Proceedings of the IVth International Conference on Baryon Resonances, edited by N. Isgur, Toronto, 1980, p. 439.

[2] S. Okubo, Phys. Lett. **5**, 165 (1963); Phys. Rev. D **16**, 2336

(1977); J. Iizuka, K. Okada, and O. Shito, Prog. Theor. Phys. **35**, 1061 (1966); J. Iizuka, Suppl. Prog. Theor. Phys. **37-38**, 21 (1966).

[3] A. De Rújula, H. Georgi, and S.L. Glashow, Phys. Rev. D **12**, 147 (1975).

[4] N. Isgur, Phys. Rev. D **12**, 3770 (1975); **13**, 122 (1976).

[5] H. Fritzsch and P. Minkowski, Nuovo Cimento A **30**, 393 (1975).

[6] There is an interesting subtlety associated with this decomposition. Figure 2(b) includes time orderings in which the pair creation occurs before the annihilation (see Fig. 3) corresponding to meson loop processes. However, the complete set of meson loop processes produce not only Fig. 2(b) but also Z graphs of Fig. 2(a) and graphs with closed $q\bar{q}$ loops inserted into Fig. 2(a). Thus a consistent treatment actually requires that S be not just the simple valence graph shown, but also include graphs with internal $q\bar{q}$ loops [4].

[7] M. Gell-Mann, R.J. Oakes, and B. Renner, Phys. Rev. **175**, 2195 (1968); S. Weinberg, Phys. Rev. D **12**, 3583 (1975).

[8] Y. Nambu, Phys. Rev. Lett. **4**, 380 (1960); J. Goldstone, Nuovo Cimento **19**, 154 (1961).

[9] A.M. Polyakov, Phys. Lett. **59B**, 82 (1975); Nucl. Phys. **B121**, 429 (1977); A.A. Belavin, A.M. Polyakov, A. Schwartz, and Y. Tyupkin, Phys. Lett. **59B**, 85 (1975); C. Callan, R. Dashen, and D.J. Gross, *ibid.* **63B**, 334 (1976); R. Jackiw and C. Rebbi, Phys. Rev. Lett. **37**, 172 (1976).

[10] G. 't Hooft, Phys. Rev. Lett. **37**, 8 (1976); Phys. Rev. D **14**, 3432 (1976).

[11] E. Witten, Nucl. Phys. **B149**, 285 (1979); **B256**, 269 (1979).

[12] G. Veneziano, Nucl. Phys. **B159**, 213 (1979).

[13] G. 't Hooft, Nucl. Phys. **B72**, 461 (1974); E. Witten, *ibid.* **B160**, 57 (1979).

[14] The extraction of the OZI amplitudes from the data can be complex. If A_{OZI} is small, $\omega-\phi$-like mixing is small as is mixing to excited nonets and glueballs, so A_{OZI} may readily be extracted from the relation $m_{I=0}=m_{I=1}+2A_{OZI}$. Note that since this extraction is in the $SU(2)_f$ sector, issues of $SU(3)$ breaking do not arise. Also note that the relation between A_{OZI} and $\mathbf{A}_{OZI}$ defined by the analogous $(\text{mass})^2$ formula $m^2_{I=0}=m^2_{I=1}+2\mathbf{A}_{OZI}$ is simply $A_{OZI}=\mathbf{A}_{OZI}/2m_{I=1}$ at the light quark mass scale. When A_{OZI} is large, mixing and $SU(3)$ breaking can become important. In such circumstances, no simple comparison to the data can be made without further assumptions. Since excited nonets will normally be 0.5 to 1.0 GeV away, when A_{OZI} is as large as it is in the pseudoscalars and scalars, the validity of ignoring internonet mixing is certainly questionable. If one nevertheless makes this assumption, then in the $SU(3)$ limit one would have $m_0=m_{I=1}+3A_{OZI}$ or alternatively $m_0^2=m_{I=1}^2+3\mathbf{A}_{OZI}$ where m_0 is the mass of the $SU(3)$ singlet meson, leading to the relation $A_{OZI}=\mathbf{A}_{OZI}/[m_0+m_{I=1}]$. For weak $SU(3)$ breaking these formulas simply become $m_0'=2m_{I=1/2}-m'_{I=0}+3A_{OZI}$ and $m_0'^2=2m^2_{I=1/2}-m'^2_{I=0}+3\mathbf{A}_{OZI}$ where now m_0' and $m'_{I=0}$ are the masses of the mainly singlet and mainly octet mesons (e.g., the η' and the η, respectively). It is this latter formula that is commonly used in defining $\mathbf{A}^{0^{-+}}_{OZI}$ in the Witten-Veneziano formula [11,12] and which leads to $3\mathbf{A}^{0^{-+}}_{OZI}=(0.85\ \text{GeV})^2$. These broken $SU(3)$ relations lead to

$$A_{OZI}=\left[\frac{\frac{m_0'+m'_{I=0}}{2}-m_{I=1/2}}{\frac{m_0'^2+m'^2_{I=0}}{2}-m^2_{I=1/2}}\right]\mathbf{A}_{OZI}.$$

The inaccuracy of these formulas from both internonet mixing and higher order corrections in $SU(3)$ breaking are not obviously small. Thus, given the dynamical assumptions required to relate a large value of A_{OZI} to observed masses, the empirical value of $A^{0^{-+}}_{OZI}$ (or $\mathbf{A}^{0^{-+}}_{OZI}$) is quite uncertain (as is $A^{0^{++}}_{OZI}$ and $\mathbf{A}^{0^{++}}_{OZI}$) and therefore only semiquantitative statements about these amplitudes can be made at this time. To convert the lattice propagator data for $\mathbf{A}_{OZI}$ to A_{OZI} in Table II for comparison to the A_{OZI} quoted in Table I, we note that in the single flavor case considered, if we once again make the assumption of small mixing with other states, the mass and $(\text{mass})^2$ formulas are $m=m_{I=1}+A_{OZI}$ and $m^2=m^2_{I=1}+\mathbf{A}_{OZI}$. (Note that we have identified the mass without the annihilation amplitude as being the $I=1$ mass that would be found for two or more flavors.) It follows that $A_{OZI}=\sqrt{m^2_{I=1}+\mathbf{A}_{OZI}}-m_{I=1}$. For small A_{OZI} this relation gives $A_{OZI}\simeq\mathbf{A}_{OZI}/2m_{I=1}$ and (as in our extraction of these quantities from the data) in this case our assumption of small mixing is justified. For large A_{OZI} such an assumption is probably not good; however, the lattice relation can be systematically improved by measuring additional elements of the mass and $(\text{mass})^2$ matrices should such an improvement be justified by an improvement in the relevant experimental data.

[15] H.J. Lipkin, Nucl. Phys. **B291**, 720 (1987); Phys. Lett. B **179**, 278 (1986); Nucl. Phys. **B244**, 147 (1984); Phys. Lett. **B124**, 509 (1983).

[16] There is a loophole in this argument. It is possible that instead there could be a conspiracy between the hadronic loop processes and other sources of OZI violation.

[17] P. Geiger and N. Isgur, Phys. Rev. D **44**, 799 (1991); Phys. Rev. Lett. **67**, 1066 (1991); Phys. Rev. D **47**, 5050 (1993); P. Geiger, *ibid.* **49**, 6003 (1994).

[18] L. Micu, Nucl. Phys. **B10**, 521 (1969); A. Le Yaouanc, L. Oliver, O. Pene, and J.-C. Raynal, Phys. Rev. D **8**, 2233 (1973); Phys. Lett. **71B**, 397 (1977); **72B**, 57 (1977); W. Roberts and B. Silvestre-Brac, Few Body Syst. **11**, 171 (1992); P. Geiger and E.S. Swanson, Phys. Rev. D **50**, 6855 (1994); R. Kokoski and N. Isgur, *ibid.* **35**, 907 (1987); Fl. Stancu and P. Stassart, *ibid.* **38**, 233 (1988); **39**, 343 (1989); **41**, 916 (1990); **42**, 1521 (1990); S. Capstick and W. Roberts, *ibid.* **47**, 1994 (1993); **49**, 4570 (1994); E.S. Ackleh, T. Barnes, and E.S. Swanson, *ibid.* **54**, 6811 (1996); and for a recent and detailed description of the implications of the $^3P_0$ model for mesons, see T. Barnes, F.E. Close, P.R. Page, and E.S. Swanson, *ibid.* **55**, 4157 (1997).

[19] C. Schmid, D.M. Webber, and C. Sorensen, Nucl. Phys. **B111**, 317 (1976); E.L. Berger and C. Sorensen, Phys. Lett. **62B**, 303 (1976).

[20] Unfortunately, Ref. [17] did not check the loop contribution to $A^{0^{-+}}_{OZI}$ since the $U_A(1)$ anomaly guaranteed that OZI violation in this sector would be large so that there was no second order paradox to evade. However, given the identified mechanism of the suppression of the loop diagrams, there is every reason to

suppose that the loop contribution to $A^{0^{-+}}_{OZI}$ is as small as in any other nonet with $J^{PC}\neq 0^{++}$.

[21] Y. Kuramashi, M. Fukugita, H. Mino, M. Okawa, and A. Ukawa, Phys. Rev. Lett. **72**, 3448 (1994).

[22] W. Bardeen, A. Duncan, E. Eichten, and H. Thacker, Nucl. Phys. B (Proc. Suppl.) **73**, 243 (1999).

[23] W. Bardeen, A. Duncan, E. Eichten, N. Isgur, and H. Thacker, hep-lat/0106008.

[24] W. Bardeen, A. Duncan, E. Eichten, and H. Thacker, Phys. Rev. D **62**, 114505 (2000).

[25] A.X. El-Khadra, G.M. Hockney, A.S. Kronfeld, and P.B. Mackenzie, Phys. Rev. Lett. **69**, 729 (1992).

[26] One can determine the ρ, a_0, and a_1 masses from chirally extrapolated fits to our data on the valence (i.e., isovector) propagators associated with Fig. 2(a), which give $m_\rho \simeq 0.8$ GeV, $m_{a_1}\simeq 1.4$ GeV, and $m_{a_0}\simeq 1.6$ GeV. The latter two masses seem to be too high. It is quite possible that they are especially sensitive to quenching since both the a_1 and the a_0 have (or are predicted to have) very strong *S*-wave couplings to nearby thresholds. [See, for example, R. Kokoski and N. Isgur, Phys. Rev. D **35**, 907 (1987); N. Isgur, *ibid.* **57**, 4041 (1998).] We have found no other recent lattice measurements of these masses close to the chiral limit (see, however, Ref. [27]), or of other spectroscopic properties of the *P*-wave mesons, and consequently hope to report on their spectroscopy in a forthcoming publication. In any event, at the level of accuracy relevant to the results reported here, these 10% effects are not significant.

[27] UKQCD Collaboration C. Michael, M.S. Foster, and C. McNeile, Nucl. Phys. B (Proc. Suppl.) **83-84**, 185 (2000).

[28] W. Lee and D. Weingarten, Nucl. Phys. B (Proc. Suppl.) **63**, 194 (1998); **73**, 249 (1999); Phys. Rev. D **61**, 014015 (2000). See also Ref. [27] on $^3P_0$-glueball mixing.

[29] The dual topological expansion is very closely related to the large N_c expansion. See G.F. Chew and C. Rosenzweig, Nucl. Phys. **B104**, 290 (1976); G. Veneziano, in Proc. 9th Ecole d'Eté de Physique des Particules, Gif-sur-Yvette, 1977, Vol. 2, p. 23.

[30] R. Dashen and A. Manohar, Phys. Lett. B **315**, 425 (1993); **315**, 438 (1993); R. Dashen, E. Jenkins, and A. Manohar, Phys. Rev. D **49**, 4713 (1994); **51**, 2489 (1995).

[31] Elizabeth Jenkins and Richard F. Lebed, Phys. Rev. D **52**, 282 (1995).

[32] E. Witten, Nucl. Phys. **B149**, 285 (1979) on p. 286.

[33] For a review, see T. Schäfer and E. Shuryak, Rev. Mod. Phys. **70**, 323 (1998).

[34] For a review, see J. Negele, Nucl. Phys. B (Proc. Suppl.) **73**, 92 (1999).

[35] John F. Donoghue and Harald Gomm, Phys. Rev. D **28**, 2800 (1983).